Available online at www.sciencedirect.com
SCIENCE DIRECT
Geochimica et Cosmochimica Acta 70 (2006) 3387–3400
Geochimica
www.elsevier.com/locate/gca

Germanium isotopic variations in igneous rocks and marine sediments

Olivier Rouxel [a,*], Albert Galy [b], Henry Elderfield [b]

[a] Woods Hole Oceanographic Institution, Marine Chemistry and Geochemistry Department, Woods Hole, MA 02543, USA
[b] Department of Earth Sciences, University of Cambridge, Downing Street, Cambridge CB2 3EQ, UK

Received 1 August 2005; accepted in revised form 27 April 2006

Abstract

A new technique for the precise and accurate determination of Ge stable isotope compositions has been developed and applied to silicate rocks and biogenic opal. The analyses were performed using a continuous flow hydride generation system coupled to a MC-ICPMS. Samples have been purified through anion- and cation-exchange resins to separate Ge from matrix elements and eliminate potential isobaric interferences. Variations of $^{74}Ge/^{70}Ge$ ratios are expressed as $\delta^{74}Ge$ values relative to our internal standard and the long-term external reproducibility of the data is better than 0.2‰ for sample size as low as 15 ng of Ge. Data are presented for igneous and sedimentary rocks, and the overall variation is 2.4‰ in $\delta^{74}Ge$, representing 12 times the uncertainty of the measurements and demonstrating that the terrestrial isotopic composition of Ge is not unique. Co-variations of $^{74}Ge/^{70}Ge$, $^{73}Ge/^{70}Ge$ and $^{72}Ge/^{70}Ge$ ratios follow a mass-dependent behaviour and imply natural isotopic fractionation of Ge by physicochemical processes. The range of $\delta^{74}Ge$ in igneous rocks is only 0.25‰ without systematic differences among continental crust, oceanic crust or mantle material. On this basis, a Bulk Silicate Earth reservoir with a $\delta^{74}Ge$ of 1.3 ± 0.2‰ can be defined. In contrast, modern biogenic opal such as marine sponges and authigenic glauconite displayed higher $\delta^{74}Ge$ values between 2.0‰ and 3.0‰. This suggests that biogenic opal may be significantly enriched in light isotopes with respect to seawater and places a lower bound on the $\delta^{74}Ge$ of the seawater to +3.0‰.This suggests that seawater is isotopically heavy relative to Bulk Silicate Earth and that biogenic opal may be significantly fractionated with respect to seawater. Deep-sea sediments are within the range of the Bulk Silicate Earth while Mesozoic deep-sea cherts (opal and quartz) have $\delta^{74}Ge$ values ranging from 0.7‰ to 2.0‰. The variable values of the cherts cannot be explained by binary mixing between a biogenic component and a detrital component and are suggestive of enrichment in the light isotope of diagenetic quartz. Further work is now required to determine Ge isotope fractionation by siliceous organisms and to investigate the effect of diagenetic processes during chert lithification.

1. Introduction

Germanium is a trace element in the Earth's crust, averaging about 1 ppm in whole rocks and minerals. Because of nearly identical ionic radii and electron configurations for germanium (Ge) and silicon (Si), the crustal geochemistry of Ge is dominated by a tendency to replace Si in the lattice sites of minerals (Goldschmidt, 1958; De Argollo and Schilling, 1978). These two elements exist in seawater as similar hydroxyacids, i.e., $Ge(OH)_4$ and $Si(OH)_4$ (Pokrovski and Schott, 1998) and the uptake and regeneration profile of Ge is similar to that of Si (Froelich and Andreae, 1981), thus providing an interesting tracer for biogenic silica cycling in the ocean.

The average Ge/Si ratio in the global ocean is about 0.7×10^{-6} (atom/atom) (Froelich and Andreae, 1981), which is significantly lower than the Ge/Si in basaltic rocks averaging about $2.6 \pm 0.3 \times 10^{-6}$ (De Argollo and Schilling, 1978). Because the two dominant Si and Ge sources to the oceans carry very different Ge/Si signatures, with $(Ge/Si)_{rivers}$ $\sim 0.54 \times 10^{-6}$ (Froelich et al., 1992) and $(Ge/Si)_{hydrothermal}$ ~ 8–14×10^{-6} (Mortlock et al., 1993), it has been proposed that the Ge/Si ratio buried in siliceous tests on the seafloor reflects the present and past source strength of river fluxes relative to hydrothermal fluxes (Shemesh et al., 1989; Froelich et al., 1992; Elderfield and Schultz, 1996). However, the use of Ge/Si as a paleoceanographic tool remains uncertain as Ge may be removed from

* Corresponding author. Fax: +1 508 457 2193.
E-mail address: orouxel@whoi.edu (O. Rouxel).

0016-7037/$ - see front matter © 2006 Elsevier Inc. All rights reserved.
doi:10.1016/j.gca.2006.04.025

the oceans in iron-rich reducing sediments independent of Si (King et al., 2000; Hammond et al., 2000; McManus et al., 2003). Based on the significant Ge isotope fractionation observed during experimental adsorption of Ge onto Fe-oxides (Galy et al., 2002), it is anticipated that Ge isotopes may provide useful geochemical tracers for the study of oceanic systems and weathering environments that can be used in addition to Ge/Si ratio systematics.

Germanium has five naturally occurring isotopes ^{70}Ge, ^{72}Ge, ^{73}Ge, ^{74}Ge and ^{76}Ge with relative abundances of 21.2%, 27.7%, 7.7%, 35.9% and 7.5%, respectively. Early investigations of Ge isotopic compositions using thermal ionisation mass spectrometry (TIMS) were limited to an uncertainty of several per mill (Shima, 1963; Green et al., 1986) and no significant variations in Ge isotope composition were found. Over the past few years, advances have been made for high precision measurement of isotopic compositions by the development of multiple collector magnetic sector inductively coupled plasma mass spectrometry (MC-ICP-MS) (Halliday et al., 1995). Hirata (1997) and Xue et al. (1997) analysed the isotopic composition of Ge of meteoritic materials by ICP-MS and identified the first direct evidence for mass fractionation of Ge isotopes. Although further analytical development has been made recently to evaluate inherent instrumental artefacts in the analysis of Ge isotopes (Galy et al., 2003), the natural variations of Ge isotopes on Earth remains unknown, mainly due to the lack of suitable analytical techniques to analyse a silicate matrix.

In this study, we present a new technique for the precise determination of Ge isotopes in various geological matrices, including silicates. The technique involves (1) chemical purification of Ge through anion-exchange and cation-exchange chromatographic columns; (2) gaseous hydride introduction into the plasma torch (HG); (3) measurement of Ge isotope ratios by MC-ICP-MS; (4) correction of instrumental mass fractionation using the standard-sample bracketing approach. The Ge isotope composition of mantle-derived rocks is presented in order to characterize the Bulk Silicate Earth reservoir. Preliminary data for modern marine sponges and authigenic glauconite have been used to assess the Ge isotope composition of seawater. Due to the high potential of using Ge isotopes as tracers in oceanic systems, we have investigated the Ge isotope compositions of marine sediments along a 500 m profile in oceanic crust in the Western Pacific (ODP Sites 1149 and 801). Sites 1149 and 801 are reference sites in the Cretaceous and Jurassic oceanic crust and offer an interesting opportunity to study Ge/Si and Ge isotopes patterns of deep-sea clays and cherts of various ages, depth and diagenetic grade.

2. Experimental

2.1. Reagents and standard

Water was purified using a Millipore deionizing system. In-house quartz-distilled nitric acid was used for the chemical separation and HG. For sample dissolution, Suprapur© hydrofluoric acid (Merck-Eurolab) has been used. All glassware and Teflon© (PTFE) materials were cleaned with 50% concentrated analytical reagent grade nitric acid and distilled water before use. 0.27 N sodium borohydride (Merck-Eurolab) solution was freshly prepared for each analytical session without filtration and was stabilized in 0.0125 N NaOH. An in-house Ge standard solution, hereafter referred to as Ge_{cam} was obtained from Aldrich (Milwaukee, WI, USA) available as 1000 μg/g Ge solution in 2% KOH.

2.2. Chemical purification of geological samples

Less than 100 mg of sample was accurately weighed into a 7 ml PTFE digestion vessel. Samples were first reacted with 2 ml of HNO_3 (50%) and taken to dryness under UV light at less than 90 °C. Total digestion of the dry residue obtained after HNO_3 dissolution was performed using 2 ml of concentrated HF. The solution was heated in the sealed PTFE containers on a hot plate at a temperature of 60 °C for more than 48 h, and solutions were shaken periodically. The solution along with precipitates were transferred into a polypropylene centrifuge tube and diluted with water to obtain a solution of ~1 N HF. Insoluble fluorides, containing mostly Ca, Mg and Al and various trace elements (Yokoyama et al., 1999) were separated from the solution by centrifugation.

The supernatant containing Ge and other soluble fluorides complexes was then loaded on an anion-exchange chromatographic column AG1-X8 (Bio-Rad, Hercules, CA, USA) filled with 1.8 ml of resin (wet volume), previously washed with 1.4 N HNO_3 and conditioned with 1 N HF. After adsorption of Ge on the column, 5 ml of 1 N HF and 2 ml of H_2O was passed through the column to elute the remaining matrix. Germanium was then eluted using 6 ml of 1.4 N HNO_3 and the solution taken to dryness under a UV lamp. Under these conditions, Ge is quantitatively recovered as well as other elements, presumably Al and Ti, whereas other matrix elements, including Fe, Si and isobaric interference Zn are eluted. Other hydride forming elements such as Se which creates isobaric interferences on ^{74}Ge and ^{76}Ge are not retained on the resin whereas As has been found to have a K_D too close to the K_D value of Ge to be fully separated. After evaporation, the solid residue was dissolved in 1.5 ml of 0.14 N HNO_3 and then loaded on a cation-exchange chromatographic column containing AG50-X8 resin (Bio-Rad, Hercules, CA, USA) with a resin bed volume of 2 ml. The column was regenerated with 4 N HNO_3 and conditioned with 0.14 N HNO_3. The solution that passed through the column contains Ge whereas residual matrix elements (including Al and Ti and any residual Zn) are strongly adsorbed on the resin. Complete recovery of Ge is assured after washing the column with 3 ml of 0.14 N HNO_3.

2.3. HG-MC-ICP-MS isotope ratio measurement

The generation of Ge hydride (GeH_4), germane, is the most suitable technique for on-line separation and speciation of ng to pg amounts of Ge (Dedina and Tsalev, 1995; Mortlock and Froelich, 1996). Since the end-product of the chemical purification of Ge is a nitric acid solution, germane has been generated using a diluted HNO_3 medium (0.14 N), which is close to the optimum condition in terms of analytical sensitivity. The use of HCl has to be avoided because of Ge chloride volatility during sample storage and isobaric interference of Cl_2 on ^{70}Ge, ^{72}Ge and ^{74}Ge.

The continuous flow HG system used for Ge isotope analysis is similar to the system used for Se (Rouxel et al., 2002) and Sb (Rouxel et al., 2003b) isotope determination. Operating parameters are presented in Table 1. A peristaltic pump was used to deliver the reducing agent and the sample to the HG system. For the gas–liquid separator, a modified Scott-type spray chamber cooled at 4 °C, without the nebulizer in place was used. The remaining aerosols are quantitatively removed by a PTFE filter and the Ge hydrides are transported with Ar via Teflon tubing directly to the ICP torch. Stability of the hydride formation was improved by using a mixing coil (20 cm), consistent pumping of the liquid waste to the drain, and by a second Ar inlet placed between the gas–liquid separator and the ICP-MS torch.

Germanium concentration and isotope ratios were measured using a Nu Instruments MC-ICP-MS. The instrumental operating conditions and data acquisition parameters are essentially those used in previous studies of Ge isotopes (Galy et al., 2003). The zero signal level correction was made for each block of 10 data (10 s of counting time) by deflecting the ion beam away from the detector. The isotopic results are reported in the same manner as proposed by Galy et al. (2003) which involves the measurement of the Ge_{cam} standard solution, before and after each sample. Each data point given in this study corresponds to the mean of three replicate measurements of individual bracketed samples. Ge_{cam} and samples were analysed within 20% of the same concentration. Between measurement of the two solutions, decontamination of the inlet was carried out using a 2% solution of HNO_3 for 5 min, which lowers cross-contamination to <0.5% of the previous Ge intensity measured and does not require any specific correction.

Under typical conditions, a minimum of 3 mL of solution was analysed at a concentration ranging from 5 to 20 ppb, generating a total Ge signal of 1.6×10^{-9} A/ppm. The amount of Ge used per analysis varied between 15 and 50 ng for most data presented in this study.

Table 1
HG-MC-ICPMS operating conditions

Inductively coupled plasma	
RF power	1300 W
Coolant Ar flow rate	13 L min^{-1}
Auxiliary Ar flow rate	1 L min^{-1}
Mass spectrometer	
Interface cones	Nickel
Acceleration voltage	4 kV
Detector/Amplifier	Faraday/$10^{11}\Omega$
Hydride generation	
Reducing agent	$NaBH_4$ (0.27 N) mixed with NaOH (1.25×10^{-2} N)
Flow rate of reducing agent	0.3 mL min^{-1}
Flow rate of sample	0.3 mL min^{-1}
Flow rate of carrier gas 1 (Ar)	0.9 L min^{-1}
Flow rate of carrier gas 2 (Ar)	9.2 L min^{-1}
Sample acidity HNO_3	0.14 N

3. Experimental results

3.1. Interferences and instrumental mass fractionation

The spectrum of the Ge isotopes suffer from molecular interferences such as $^{35}Cl^{35}Cl^+$ on $^{70}Ge^+$, $^{40}Ar^{16}O_2{}^+$, $^{36}Ar^{36}Ar^+$ on $^{72}Ge^+$, $^{58}Ni^{16}O^+$, $^{38}Ar^{36}Ar^+$ on ^{74}Ge and $^{38}Ar^{38}Ar^+$, $^{36}Ar^{40}Ar^+$ on $^{76}Ge^+$. The use of a desolvating nebulizer reduces oxygen-based interferences, and except for ^{76}Ge isotope, Ar-based isobaric interferences are undistinguishable from the intrinsic background noise of the detector system (Galy et al., 2003). Because the HG technique involves the formation of germane GeH_4 and H_2 and potentially other volatile species, we further evaluated the level of potential interferences on Ge isotopes. For several analytical sessions, we measured, , the Ge isotope composition of the standard solution at various concentrations, from 10 ppb down to 10 ppt (Fig. 1). The theoretical interference intensity on each Ge isotope can then be calculated based on the deviation of the Ge isotope ratios for the Ge_{cam} solution at different concentration. Using this method, we evaluated the interferences to be on the order of 1.7%, <0.001%, 0.002%, 0.003% and 0.004% of the typical signal of $^{76}Ge^+$, $^{74}Ge^+$, $^{73}Ge^+$, $^{72}Ge^+$ and $^{70}Ge^+$, respectively (10 ppb solution). This induces a shift of less than 17.3‰, 0.03‰, 0.02‰ and 0.01‰ in $\delta^{76}Ge$, $\delta^{74}Ge$, $\delta^{73}Ge$ and $\delta^{72}Ge$, respectively. Therefore, except for ^{76}Ge, all other Ge isotopes may be analysed without any correction for isobaric interference using the HG technique. For this reason, we discontinued measuring ^{76}Ge since it is clear that the fractionation is mass dependent. The level of the GeH^+ signal, which may produce isobaric interferences on ^{73}Ge and ^{74}Ge isotopes, has proven to be insignificant by the comparison of the signal intensity at mass 74 ($^{74}Ge^+$) and at mass 75 ($^{74}GeH^+$). Finally, although the sampler and skimmer cones are made of pure nickel, we could not detect interferences from $^{58}Ni^{16}O$ at mass 74.

As shown in Fig. 2, the Ge isotopic ratios of the Ge_{cam} standard measured by HG and desolvating nebuliser (using the same instrument) are in close agreement. The evolution of the $^{72}Ge/^{70}Ge$ and $^{74}Ge/^{70}Ge$ ratios follows

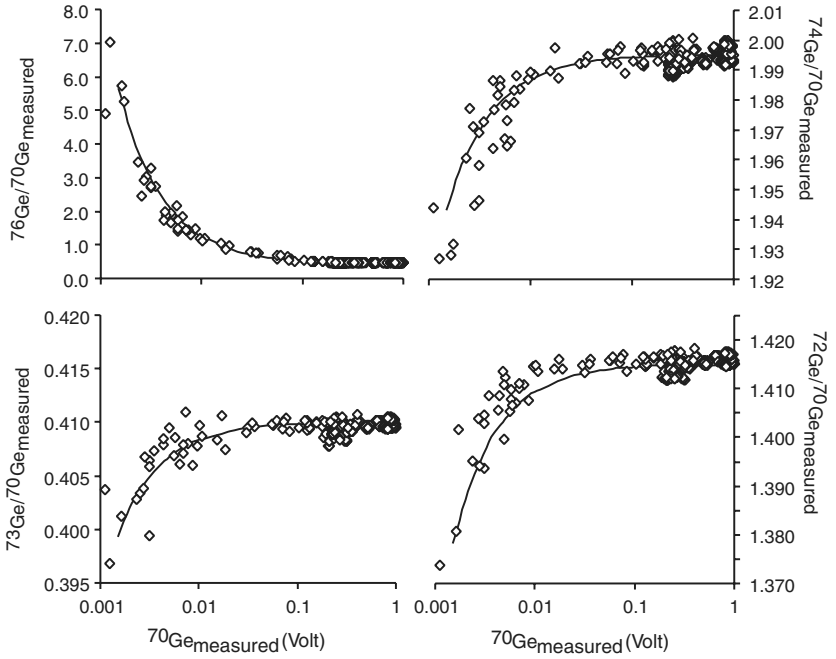

Fig. 1. Intensity of ^{70}Ge (V) in logarithm scale versus measured Ge isotope ratios. The solid line represents the regression of the data measured for different Ge concentrations of Ge_{cam} (10 ppt to 10 ppb) using hydride generation coupled to MC-ICPMS and corresponds to the contribution of background and interference levels on Ge isotope measurements. At working beam size and except for ^{76}Ge, which suffers from Ar_2^+ interference, measured Ge isotopic ratios have insignificant interference levels.

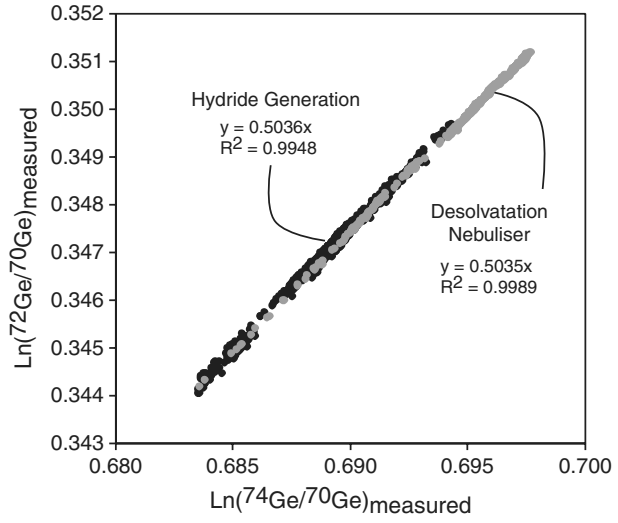

Fig. 2. Three-isotope representation of the logarithm of measured Ge isotope ratios of the Ge_{cam} standard solution using hydride generation (10 ppb solution) and desolvation system (0.2–0.5 ppm solution) as reported by Galy et al. (2003). In this graph, the theoretical relationships between the instrumental mass-dependent fractionation for the ^{72}Ge/^{70}Ge and ^{74}Ge/^{70}Ge ratios are straight lines. The relationships between the instrumental mass-dependent fractionation for the ^{72}Ge/^{70}Ge and ^{74}Ge/^{70}Ge ratios are similar using both techniques.

the same theoretical mass-dependent fractionation curve given by Galy et al. (2003) confirming further the lack of detectable isobaric interference introduced by the HG system.

3.2. Analysis of standard solutions: internal reproducibility

The precision of the standard-sample bracketing technique adopted here has been assessed from the repeatability of Ge_{cam} standard solutions measured over different analytical sessions and Ge concentrations (Table 2). For routine analysis of the Ge_{cam} solution with Ge concentrations ranging from 10 to 50 ppb, we estimated an overall precision of about 0.14‰, 0.13‰ and 0.09‰ for δ^{74}Ge, δ^{73}Ge and ^{72}Ge, respectively (84 duplicates). The quantity of Ge used per analysis was between 15 and 150 ng. Compared to a previous investigation using the desolvation system (Galy et al., 2003), the HG technique requires a 10th of the Ge with a similar long-term reproducibility.

In order to assess the minimum amount of Ge required per analysis we analysed the Ge_{cam} solution with Ge concentrations ranging from 1 to 5 ppb (Table 2), corresponding to 3–15 ng of Ge analysed. At low Ge intensity the analytical precision deteriorates, but the accuracy remains for sample sizes as low as 3 ng with a precision of about 0.1‰ per mass unit.

Two solutions previously measured against Ge_{cam} using the desolvation method and after the removal of the alkali matrix (Ge#2b and Ge#4 solutions with δ^{74}Ge values at 1 ± 0.1‰; Galy et al., 2003) have been re-measured by HG without chemical separation (Table 2). The two methods gave identical values within the analytical uncertainty. Additionally, the matrix-doping experiments presented in Table 2, show that results are not biased by the addition of Fe, Al, Na, K and Se. Therefore, one of the major advantages of the HG technique for the determination of

Table 2
Ge isotope composition of pure and matrix-doped standard solutions

	Ge (ppb)	$\delta^{74}Ge_{cam}$ (‰)	2σ	$\delta^{73}Ge_{cam}$ (‰)	2σ	$\delta^{72}Ge_{cam}$ (‰)	2σ
Standard solution "Ge_{cam}"							
($N = 3$)	1.0	−0.06	0.35	−0.38	0.97	−0.04	0.27
($N = 3$)	2.0	−0.05	0.19	0.03	0.47	−0.10	0.10
($N = 3$)	4.0	0.02	0.20	−0.04	0.35	0.02	0.23
($N = 3$)	5.0	0.11	0.08	0.08	0.23	0.04	0.08
($N = 27$)	10	0.00	0.13	0.00	0.13	0.00	0.08
($N = 17$)	20	0.02	0.14	0.01	0.11	0.01	0.09
($N = 19$)	30	0.01	0.13	0.01	0.09	0.00	0.06
($N = 21$)	50	0.00	0.11	0.01	0.10	0.00	0.06
($N = 8$)	100	0.00	0.15	0.00	0.09	0.00	0.10
Miscellaneous							
Ge#2b[a]	20	1.08	0.08	0.83	0.12	0.54	0.04
Duplicate	20	1.13	0.12	0.83	0.10	0.58	0.05
Ge#4[b]	20	1.02	0.21	0.78	0.12	0.52	0.15
Ge_{cam} doped with elemental solution without chemical purification							
Se 10 ppb	10	0.04	0.19	−0.01	0.18	−0.01	0.10
Al 100 ppb	10	−0.02	0.20	−0.08	0.23	−0.02	0.09
Na 100 ppb	10	0.05	0.14	0.05	0.08	0.02	0.09
K 100 ppb	10	0.09	0.21	0.06	0.08	0.03	0.12
Fe 100 ppb	10	0.09	0.03	0.10	0.09	0.02	0.00
Fe 200 ppb	10	0.07	0.18	0.00	0.05	0.04	0.12

[a] $\delta^{74}Ge = 1.08‰$ (Galy et al., 2003).
[b] $\delta^{74}Ge = 0.94‰$ (Galy et al., 2003).

Ge isotopes, in addition to the increase in sensitivity, is the lack of any matrix effects, in particular from alkalis. Selenium is a well-known hydride forming element but the yield of Se hydride formation in a HNO_3 medium is very low and no interference (on ^{74}Ge) is observed from Se at Ge/Se close to unity. In addition, Se is successfully separated through chemical purification. Because germane formation may be sensitive to matrix effects such as metals at high concentration (Dedina and Tsalev, 1995), we always purify natural samples to obtain a sample matrix close to that of standard.

Through the chemical purification of Ge described above, a significant fraction (>50%) of As in a sample remains in the Ge fraction after the chemical purification. Arsenic is a well-known hydride forming element and As/Ge ratios in natural samples may vary greatly, for example, from 0.1 in basalts to >10 in marine sediments. Therefore, the effect of As concentration on Ge isotopic composition has been evaluated by doping the Ge_{cam} solution with variable amounts of As (Fig. 3). The Ge isotope compositions of As-doped solutions gave consistent results within the analytical uncertainties showing that As (to a level of up to 50 times the Ge concentration) does not interfere in Ge hydride formation or changes instrumental mass fractionation. Furthermore, the use of HNO_3 as a reaction medium strongly suppresses the formation of As hydrides. Nevertheless, intensity at mass 75 was carefully monitored for all samples with an unknown As content.

3.3. External reproducibility

The overall accuracy of the analytical procedure has been verified by the "standard-addition" method applied for the measurement of Ge concentration and Ge isotope

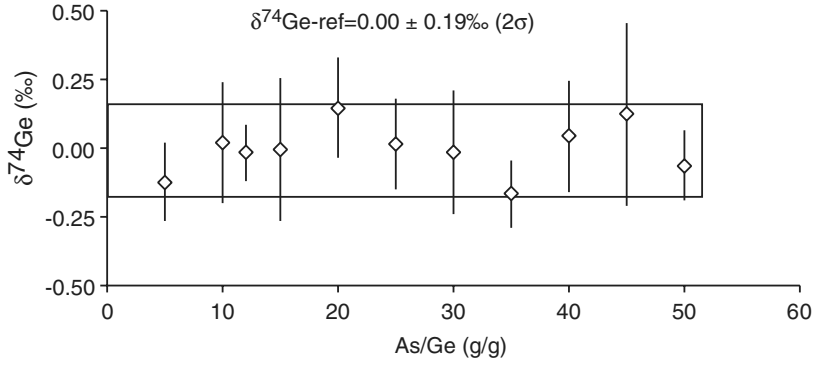

Fig. 3. Assessment of any matrix effects from As on the Ge isotope ratios. Arsenic-doped Ge solutions are measured against a pure Ge solution and expressed in δ-unit. No Ge isotopic shift is observed within analytical uncertainty for As concentrations of up to 500 ppb in a 10 ppb Ge solution.

composition of BHVO-1 (USGS, Hawaiian basalt). Prior to sample dissolution and chemical purification, 100 mg of BHVO-1 were doped with various amounts of the Ge_{cam} standard (between 0 and 350 ng). The Ge concentration and Ge isotope composition of these composite samples were measured and results are presented in Fig. 4. The relationship between the concentration of total Ge in the sample and the theoretical concentration of Ge added shows an overall yield of the chemical purification of $100 \pm 5\%$ and a Ge concentration of 1.44 ± 0.1 ppm in BHVO-1. The recovery of Ge from a silicate matrix is, thus, quantitative. The concentration of Ge in BHVO-1 compares well with the literature value (Table 3). The relationship between δ^{74}Ge values for the composite sample and the percentage of Ge added in BHVO-1 follows the predicted mixing relationship with the δ^{74}Ge value of BHVO-1 estimated to be $1.38 \pm 0.10‰$ (Fig. 4). The contribution of Ge from the whole procedural chemistry blank was measured for each batch of samples ($n = 12$) and has been found to be in all cases below 10 pg and indistinguishable from the instrumental blank.

The external reproducibility of our method has been evaluated through the replicate measurements of standard solutions Ge_{cam} and georeference material BHVO-1 processed through the complete chemical preparation, including digestion step and chromatography separation. The effect of Ge loss due to insoluble fluoride precipitation or silica gel formation has been further assessed by dissolving various amounts of BHVO-1 (sample weight varying from 10 to 150 mg, corresponding to Ge amount of 16–240 ng) with the same quantity of concentrated HF (2 mL). Results presented in Fig. 5 show that no significant Ge isotope deviation is observed for sample weights of up to 150 mg. Duplicate measurements of BHVO-1 give consistent results with a δ^{74}Ge value of $1.27 \pm 0.18‰$, within error of the δ^{74}Ge obtained using the standard-addition method. The overall external analytical precision for δ^{74}Ge, δ^{73}Ge and δ^{72}Ge is, thus, estimated to be 0.20‰, 0.20‰ and 0.15‰, respectively. This precision is confirmed by duplicate measurements of various geological samples presented below. These samples cover a range a Ge concentrations, rock type and matrix.

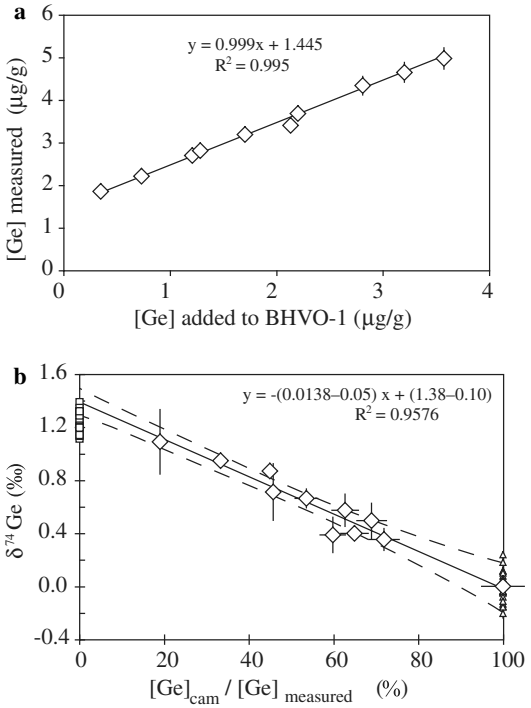

Fig. 4. Ge concentration (a) and Ge isotope composition (b) of synthetic samples obtained by doping BHVO-1 (basalt) with various amount of Ge_{cam}. Based on the regression coefficient of the relationship in (a), the yield of the chemical purification is $99.9 \pm 5\%$. The extrapolated Ge concentration of BHVO-1 of 1.45 ppm compares well with reported data (from 1.45 to 1.64 ppm) for this reference material and its δ^{74}Ge is estimated to be $1.38 \pm 0.1‰$, undistinguishable from duplicate measurement of un-doped BHVO-1. Note that the regression of the standard-addition experiment passes through the duplicate analysis (i.e., chemical purification and isotopic measurements) of Ge_{Cam} (triangles) and BHVO-1 (squares).

4. Material

This work primarily involves analyses of georeference materials (Govindaraju, 1994) and other natural samples representing important geochemical reservoirs (i.e., continental and oceanic basalts, granites, deep-sea sediments and marine siliceous organisms). We also analysed marine sediments in depth profiles from ODP Sites 801 and 1149 drilled during ODP Leg 129 (Larson et al., 1992) and Leg 185 (Plank et al., 2000) in Jurassic and Cretaceous Pacific oceanic crust (Table 4) to investigate Ge isotope systematics in various lithologies such as deep-sea clays and cherts. Both sites are located in the West Pacific seaward of the Mariana and Izu-Bonin trenches. A complete lithostratigraphic section of sediments at Sites 1149 and 801 is presented in Plank et al. (2000) and Rouxel et al. (2003a).

5. Results and discussion

5.1. Germanium isotope composition of the Bulk Silicate Earth

A crude estimate of the Ge isotopic composition of the Bulk Silicate Earth (BSE) has been obtained by the analysis of various mantle-derived rocks such as tholeiitic glasses from mid-ocean ridges, continental and volcanic islands basalts, peridotite and granite. Germanium isotopic results, together with Ge concentrations and Ge/Si ratios are presented in Table 3 and Fig. 6. Although the samples investigated are not necessarily the best representatives of the oceanic and continental crust, the homogeneity of their δ^{74}Ge values is remarkable and allows an estimate of the δ^{74}Ge value of BSE at around $1.3 \pm 0.2‰$. In addition, the δ^{72}Ge and δ^{73}Ge values are constant and related to δ^{74}Ge values by a mass-dependent relationship within their analytical uncertainties.

Table 3
Ge isotope composition of mantle-derived rocks and georeferences material

Sample name	SiO_2[a] (wt%)	Ge (ppm) literature	Ge (ppm)	Ge/Si ($\times 10^{-6}$)	δ^{74}Ge	2σ	δ^{73}Ge	2σ	δ^{72}Ge	2σ	Description
BHVO-1	49.9	1.64[a];1.55[c]	1.57	2.6	1.27	0.10	0.97	0.21	0.68	0.10	Basalt, Hawaii (USA)
BIR-1	47.8	1.5[a];1.45[b];1.53[b]; 1.49[c];1.52[d]	1.50	2.6	1.21	0.25	0.97	0.15	0.68	0.06	Basalt (Iceland)
DV1-2	50.5		1.50	2.5	1.16	0.08	0.80	0.05	0.59	0.05	Tholeitic basalt (Mid Atlantic Ridge)
NZ-06-14	48.8		1.50	2.5	1.30	0.11	0.95	0.05	0.68	0.06	Tholeitic basalt (Pacific Ocean)
Duplicate			1.41	2.4	1.25	0.12	0.85	0.13	0.65	0.10	
Duplicate					1.14	0.09	0.91	0.05	0.64	0.04	
Oceanic crust estimate				2.5	1.22	0.11	0.91	0.15	0.65	0.08	
DNC-1	47.0	1.3[a];1.26[b]	1.29	2.3	1.29	0.16	1.03	0.21	0.70	0.11	Diabase, North Carolina (USA)
AN-G	46.3	0.8[a];0.93[c]	0.83	1.5	1.38	0.15	0.88	0.03	0.76	0.09	Anorthosite (West Greenland)
G-2	69.1	1.14[a];0.94[b];1.02[b]	1.03	1.2	1.36	0.17	1.08	0.16	0.70	0.10	Granite, Rhode Island (USA)
GH	75.8	2.0[a];2.18[c]	2.00	2.2	1.25	0.21	0.96	0.13	0.64	0.12	Granite, Hoggar (Algeria)
Continental crust estimate				1.8	1.32	0.12	0.99	0.17	0.70	0.10	
BCR-1	54.1	1.5[a];1.42[b];1.45[c]	1.50	2.3	1.16	0.03	0.82	0.07	0.58	0.08	Basalt, Columbia River Group (USA)
DTS-1	40.4	0.88[a];0.84[c]	0.87	1.8	1.25	0.12	1.07	0.30	0.63	0.14	Dunite, Washington (USA)
PCC-1	41.7	0.94[a]	0.95	1.9	1.41	0.14	1.18	0.35	0.79	0.18	Peridotite, California (USA)
Bulk Silicate Earth estimate				2.1	1.27	0.16	0.96	0.23	0.67	0.12	

[a] Govindaraju (1994).
[b] Mortlock and Froelich (1987, 1996).
[c] Halicz (1990).
[d] Kurtz et al. (2002).

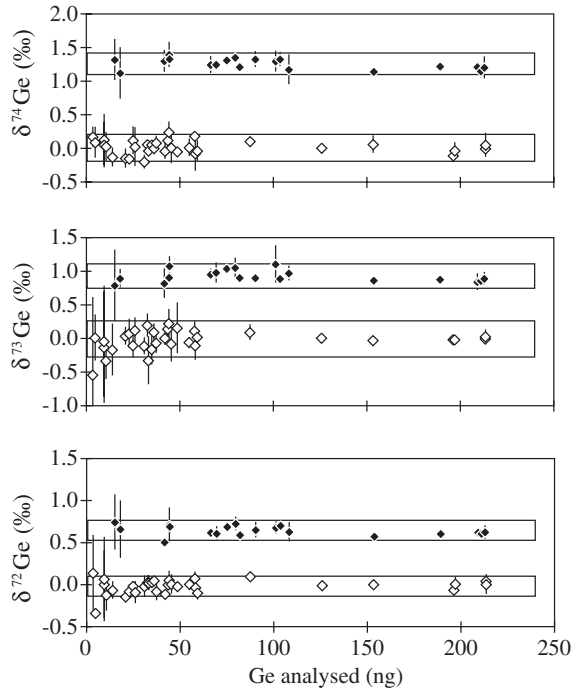

Fig. 5. Plot of δ^{74}Ge, δ^{73}Ge, δ^{72}Ge versus the quantity of Ge used per analysis (ng). Duplicated chemical purification and isotopic analysis for Ge_{cam} and BHVO-1 are reported and an overall external precision (represented as boxes in the diagrams) of 0.20‰, 0.20‰ and 0.15‰ for δ^{74}Ge, δ^{73}Ge and δ^{72}Ge values, respectively, are obtained. The precision for δ^{73}Ge values is less than for δ^{74}Ge values because ^{73}Ge is 4.7 times less abundant that ^{74}Ge and the precision is limited by counting statistics.

The average Ge/Si ratio of basalts determined around 2.5×10^{-6} is in good agreement with previous estimates based on a much larger sample set (De Argollo and Schilling, 1978; Bernstein, 1985). On the other hand, the average Ge/Si ratio of the continental crust (around 1.8×10^{-6}) is significantly higher than previous estimates (Mortlock and Froelich, 1987). Possibly, the discrepancy is due to the lithological heterogeneity of the continental crust and the limited number of samples considered here. However, the small variation in the δ^{74}Ge of continental crust materials and the lack of relationship between the Ge/Si ratio and the δ^{74}Ge suggest that our estimate of the isotopic composition of the continental crust and BSE is not significantly biased by sampling.

Given the lack of a standard reference material for the measurement of Ge isotopes, direct comparison between our estimate of the BSE and previous reported compositions of terrestrial (Green et al., 1986) and meteoritic material (Hirata, 1997; Xue et al., 1997), is difficult. It is, however, worth noting that high purity Ge solutions used during the study of meteoritic materials have a rather restricted range in isotopic composition of around 0.1‰/amu (Hirata, 1997; Xue et al., 1997; Galy et al., 2003). So, our estimate of the BSE reduces the difference between the Ge isotopic composition of iron meteorites and the BSE to less than 1‰/amu. Our value also suggests that iron meteorites have a Ge isotopic composition similar to or heavier than the BSE. Since our data do not support a significant isotopic fractionation associated with mantle-crust segregation, any differences between the Earth and iron meteorites has to be associated either with a primordial isotopic heterogeneity in the solar nebula recorded at the planetesimals scale or with volatilisation–condensation mechanisms as suggested previously by Hirata (1997).

Table 4
Chemical composition of selected marine sediments from West Pacific (ODP Site 1149 and 801) recovered during Leg 129 and 185

Sample	mbsf[a]	LOI (wt%)	Al_2O_3 (wt%)	CaO (wt%)	Fe_2O_3 (wt%)	K_2O (wt%)	MgO (wt%)	MnO (wt%)	Na_2O (wt%)	P_2O_5 (wt%)	SiO_2 (wt%)	TiO_2 (wt%)	SUM (wt%)	Stratigraphic age	Description
1149A-01H1,140[b]	1.4	9.1	14.88	3.01	5.48	1.88	2.35	0.12	3.14	0.07	58.5	0.57	99.1	Pleistocene (<0.1 Ma)	Ash and biogenic silica-bearing clay
1149A-04H2,140[b]	26.1	11.1	14.28	1.46	7.08	2.53	2.71	0.12	2.74	0.10	57.7	0.64	100.4	Pleistocene (0.8 Ma)	
1149A-05H5,140[b]	40.1	11.2	14.77	1.55	5.81	2.71	2.45	0.10	2.74	0.10	57.5	0.63	100.1	Pleistocene (1.3 Ma)	
1149A-07H4,140[b]	57.6	13.3	13.40	2.24	4.07	1.70	1.70	0.24	3.58	0.09	59.0	0.56	100.1	Pliocene (2.2 Ma)	
1149A-09H3,140[b]	75.1	10.9	14.92	2.68	7.28	2.09	2.55	0.30	3.14	0.12	56.5	0.69	100.2	Pliocene (3.2 Ma)	
1149A-12H3,140[b]	113.8	14.3	15.05	1.27	5.55	2.33	2.66	0.52	2.74	0.10	53.5	0.62	100.4	Pliocene–Miocene (6.5 Ma)	
1149A-14H2,140[b]	121.1	8.4	16.12	1.56	7.10	2.27	3.23	0.43	2.90	0.08	55.7	0.70	100.3	n.d.	Dark brown pelagic clay
1149A-16H3,140[b]	141.6	19.2	14.80	0.60	5.96	1.78	3.72	0.74	2.99	0.12	50.2	0.56	99.6	n.d.	
1149A-18H3,140[b]	160.4	15.0	17.41	0.65	7.80	3.65	3.10	1.85	1.81	0.30	49.6	0.63	99.5	n.d.	
1149A-20X1,140[b]	171.2	13.2	14.08	2.18	7.83	2.75	3.03	1.48	1.36	1.62	51.0	0.67	100.3	n.d.	
1149B-06R1,38[c]	199.1	4.2	2.08	0.30	1.77	0.50	0.57	0.09	0.36	0.14	89.7	0.11	95.6	Middle Albian (100–110 Ma)	Brown chert with well-preserved radiolarians
1149B-22R1,106[c]	341.2	2.3	1.36	0.05	0.95	0.36	0.29	0.05	0.16	0.05	94.2	0.05	97.5	Upper Valanginian (131–138 Ma)	Red chert with irregular banding
1149C-01W1,113[c]	(234.3)[d]	2.4	0.60	0.05	0.46	0.18	0.16	0.05	0.16	0.05	95.6	0.05	97.4	Unknown	Light brown peach chert
1149C-05R1,19[c]	303.0	2.7	1.02	0.33	0.86	0.31	0.31	0.14	0.19	0.05	93.9	0.05	97.1	Hauterivian (126–131 Ma)	Dark brown chert
1149D-04R1,43[c]	291.3	2.3	1.12	0.85	0.80	0.30	0.30	0.07	0.16	0.05	93.8	0.05	97.5	L. Valanginien (131–138 Ma)	Light brown chert
801B-20R1,12[c]	374.6	2.4	1.49	0.18	0.94	0.34	0.31	0.17	0.25	0.09	93.6	0.06	97.4	U. Thithonian (144–152 Ma)	Dark brown chert
801B-27R1,62[c]	415.3	4.9	4.39	0.33	3.40	1.23	1.16	0.69	0.85	0.10	82.7	0.21	95.1	Kimmeridgian (152–156 Ma)	Brown cream colored silica-rich sediment
801B-31R1,33[c]	433.9	2.6	1.65	0.18	1.28	0.43	0.33	0.25	0.28	0.09	92.6	0.08	97.2	Oxfordian (156–163 Ma)	Dark brown chert with unmineralized fractures
801B-40R1,02[c]	476.9	0.7	0.22	0.05	1.04	0.06	0.05	0.05	0.05	0.05	98.0	0.05	99.6	Callovian–Bathonian (163–176 Ma)	Dark brown chert with hydrothermal quartz

[a] Meters below seafloor.
[b] Major element data obtained by ICP-AES at Boston University (T. Plank, pers. communication) after $LiBO_2$ fusion.
[c] Major element data obtained by ICP-AES at CRPG-CNRS (SARM Service Analyse Roche et Mineraux) after $LiBO_2$ fusion.
[d] Sample from washed-core recovery operation.

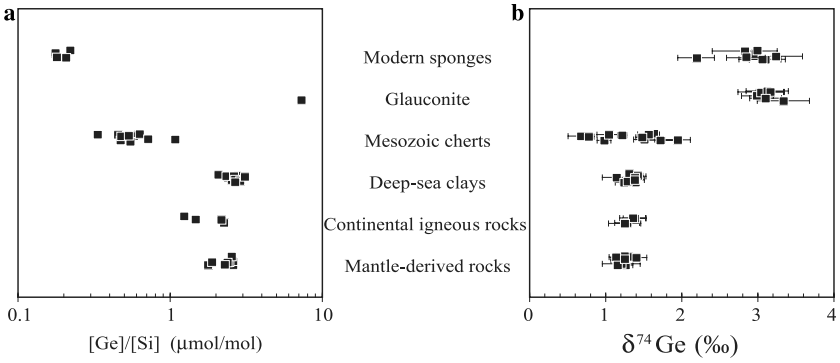

Fig. 6. Ge/Si ratios (a) and Ge isotope composition (b) of various types of rocks and marine precipitate.

5.2. Germanium isotope composition of marine sponges and glauconite

Opal sponge spicules were obtained from live sponges growing on the seafloor (Table 5). Two deep-sea specimen (NE Pacific) and one coastal marine sponge (California) have been analysed and yield similar Ge concentrations (between 0.18 and 0.26 ppm) but variable δ^{74}Ge values (between 2.4‰ and 3.1‰). These results clearly demonstrate that δ^{74}Ge values of modern marine sponges are enriched in heavy isotopes by more than ~1.0‰ relative to the BSE. Such a significant difference might be explained by (1) Ge isotopic fractionation during biomineralization by organisms and/or (2) a high δ^{74}Ge value for Ge in seawater. Sponges are considered to have a low affinity for silicic acid (Reincke and Barthel, 1997) and the inefficient silicon uptake mechanism has been suggested to explain their preferential enrichment in the light Si isotope (Douthitt, 1982; De La Rocha, 2003). The high δ^{74}Ge values obtained for marine sponges is thus at odds with the expectation from Si isotopes. However, the difference of δ^{74}Ge values of up to 0.6‰ between two deep-sea sponges from the same area are best explained by biological fractionation during Ge uptake. The relatively high δ^{74}Ge values obtained for different species at different depth also suggest that sponges likely record a Ge isotope composition of seawater above 3.0‰. This value is a lower bound of the Ge isotopic composition of modern seawater because, if sponges fractionate Ge isotopes, they likely discriminate against heavy isotopes.

Glauconite is an iron-rich authigenic clay mineral, which forms in shallow marine environments at the sedi-

Table 5
Ge isotope composition of various marine materials

Sample name	SiO_2 (wt%)	Ge (ppm)	Ge/Si ($\times10^{-6}$)	δ^{74}Ge	2σ	δ^{73}Ge	2σ	δ^{72}Ge	2σ
Glauconite[a], Normandy (France)									
GL-O	50.9	4.50	7.3	3.34	0.34	2.43	0.28	1.77	0.19
Duplicate				3.17	0.18	2.49	0.10	1.64	0.17
Duplicate[b]		4.51		3.13	0.28	2.37	0.24	1.57	0.15
Duplicate[b]		4.38		3.05	0.30	2.31	0.25	1.49	0.19
Duplicate[b]		n.d.[c]		3.10	0.19	2.36	0.13	1.49	0.10
Duplicate[b]		n.d.[c]		2.99	0.19	2.24	0.13	1.45	0.10
Deep-sea sponges (34°45′N; 123°00′W); NE Pacific, 4000 m									
Hyalonema bianchoratum, *spicule columns*									
Stalk 11	n.d.[c]	0.21	0.18[d]	2.97	0.05	2.07	0.25	1.49	0.04
Duplicate				3.10	0.21	2.28	0.38	1.67	0.20
Stalk 12	n.d.[c]	0.23	0.19[d]	3.24	0.35	2.21	0.33	1.75	0.17
Duplicate				3.06	0.30	2.39	0.72	1.58	0.23
Stalk A[b]	n.d.[c]	0.27	0.22[d]	3.00	0.24	2.26	0.14	1.46	0.14
Stalk B[b]	n.d.[c]	0.22	0.18[d]	2.85	0.24	2.11	0.14	1.42	0.14
Bathydorus laevis ssp. spinosus									
#1[b]	n.d.[c]	0.26	0.21[d]	2.20	0.24	1.56	0.14	1.08	0.14
Coastal sponge (*Axinella mexicana* sp.); California Margin									
#1	n.d.[c]	0.18	0.15[d]	2.83	0.43	1.73	0.07	1.50	0.25

[a] Georeference material GL-O, 95 Ma old glauconite (Kapusta et al., 1997), SiO_2 concentration after Govindaraju (1994).
[b] Duplicate dissolution, chemical purification and isotope analysis performed at WHOI on Neptune MC-ICPMS.
[c] Not determined.
[d] Calculated using Si concentration for pure opal.

ment–water interface within a reducing microenvironment. The retention of Ge by clay minerals is known to be the main mechanism fractionating Ge/Si ratios in the weathering environment (Kurtz et al., 2002). The Ge/Si ratio of the glauconite sample GL-O (Govindaraju, 1994) is 7.2×10^{-6}, one order of magnitude higher than the seawater ratio (Table 5) and confirms the preferential incorporation of Ge in secondary clay minerals in the marine environment. A part of Ge incorporated in glauconite may be derived from detritic materials or Ge-rich primary mineral (such as biotite). However, the high δ^{74}Ge value at 3.2‰ argues against the predominance of a terrigenous source of Ge, and suggests rather that Ge derives from seawater with a high δ^{74}Ge value. By analogy with the isotopic fractionation occurring during the Ge sorption onto Fe hydroxide (Galy et al., 2002), it is likely that authigenic minerals have a lower δ^{74}Ge values than in seawater. Because of the heavy δ^{74}Ge values of deep-sea sponges and glauconite, we suggests that seawater Ge isotopic composition may be enriched in heavy isotopes by more than 2‰ relative to BSE.

5.3. Germanium isotope variations of deep-sea marine sediments

Germanium concentrations, Ge/Si ratios and Ge isotope compositions of samples from Site 1149 and 801 are presented in Table 6. As illustrated in Fig. 7, δ^{74}Ge values of deep-sea clays, and to a lesser extent Ge/Si ratios, are homogeneous in contrast with values for deep-sea cherts. δ^{74}Ge values of deep-sea clays (1.33 ± 0.18‰) overlap with BSE, whereas Ge/Si ratios are on average 23% higher. Because deep-sea sediments are essentially composed of terrigenous materials with only minor biogenic components (siliceous organisms), it can be suggested that, as a whole, secondary clay formations during rock weathering processes do not significantly fractionate Ge isotopes.

Ge/Si ratios of deep-sea cherts vary between 0.34×10^{-6} and 1.1×10^{-6} (Table 6), on average slightly higher than found in other Mesozoic cherts, with Ge/Si ratios ranging between 0.19×10^{-6} and 0.72×10^{-6} (Kolodny and Halicz, 1988). The relationships between major element concentrations (Fig. 8) show that variable proportions of clays are present in cherts. The calculated amount of clay mineral relative to opal is generally below 10%, except for one sample (801B-27R1,62) having up to 25% of clay. This feature is typical of radiolarian cherts and porcellanites at Site 801 and elsewhere (e.g., Behl and Smith, 1992). Germanium and Al_2O_3 concentrations are poorly correlated (Fig. 8) suggesting that the variable proportion of detrital input in these cherts is not the sole cause for variable Ge/Si ratios. Binary mixing between a biogenic component and a detrital component is further ruled out by isotopic mass balance calculation because most of the δ^{74}Ge and Ge/Si values for deep-sea cherts do not plot along the mixing relationship defined between diagenetic fluids from the dissolution of biogenic opal (estimated from sponges) and clays (Fig. 9). Radiolarians are known to have provided most of the silica for the lithification of the Mesozoic deep-sea cherts (Behl and Smith, 1992) and they could have different δ^{74}Ge values than those of modern sponges [either because, like for Si (Douthitt, 1982), they have a distinct Ge isotopic fractionation factors or because of secular

Table 6
Ge isotopic composition of selected marine sediments, ODP Sites 801 and 1149

Sample	Ge (ppm)	Ge/Si[a] ($\times 10^{-6}$)	δ^{74}Ge	2σ	δ^{73}Ge	2σ	δ^{72}Ge	2σ
Red-brown deep-sea clays								
1149A-01H1,140	1.70	2.40	1.42	0.12	1.02	0.08	0.75	0.06
1149A-04H2,140	1.93	2.77	1.31	0.1	0.92	0.11	0.65	0.05
1149A-05H5,140	1.77	2.55	1.39	0.13	1.01	0.12	0.71	0.04
1149A-07H4,140	1.48	2.08	1.15	0.19	0.81	0.17	0.58	0.15
1149A-09H3,140	1.60	2.35	1.31	0.00	0.84	0.08	0.68	0.00
1149A-12H3,140	1.70	2.63	1.42	0.07	1.06	0.15	0.76	0.04
1149A-14H2,140	1.80	2.68	1.39	0.03	1.02	0.11	0.75	0.08
1149A-16H3,140	1.75	2.89	1.39	0.10	1.05	0.04	0.75	0.07
1149A-18H3,140	1.86	3.10	1.25	0.11	0.85	0.07	0.63	0.14
1149A-20X1,140	1.65	2.68	1.29	0.09	0.85	0.24	0.69	0.10
Deep-sea cherts and radiolarites								
1149B-06R1,38	0.49	0.46	0.68	0.17	0.59	0.16	0.38	0.05
1149B-22R1,106	0.70	0.62	1.51	0.14	1.22	0.07	0.83	0.10
Duplicate	0.66	0.58	1.64	0.01	1.19	0.09	0.85	0.07
Duplicate	0.72	0.63	1.57	0.14	1.25	0.08	0.82	0.00
1149C-01W1,113	0.39	0.34	1.22	0.06	1.02	0.06	0.66	0.03
1149C-05R1,19	0.62	0.55	1.48	0.08	1.21	0.09	0.77	0.05
1149D-04R1,43	0.54	0.47	1.72	0.22	1.16	0.19	0.85	0.12
801B-20R1,12	0.54	0.48	0.78	0.07	0.61	0.09	0.39	0.03
801B-27R1,62	1.08	1.08	0.98	0.09	0.82	0.06	0.52	0.05
801B-31R1,33	0.6	0.54	1.04	0.15	0.86	0.13	0.54	0.09
801B-40R1,02	0.85	0.72	1.95	0.17	1.78	0.25	1.04	0.10

[a] Calculated using Si concentration in Table 4.

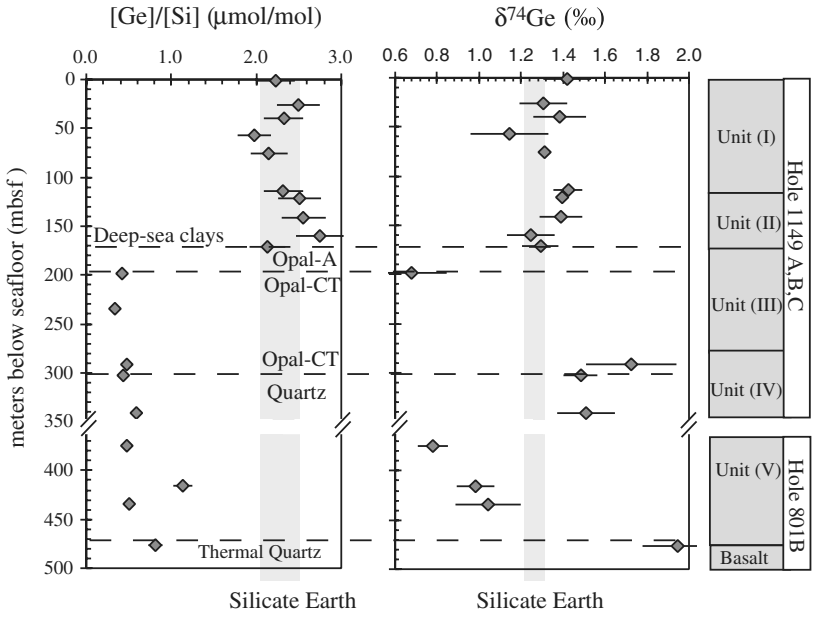

Fig. 7. Stratigraphic section in meters below seafloor through the first 350 m of the sediment section at ODP Site 1149 and the last 150 m of the sediment section at ODP Site 801. Ge/Si and δ^{74}Ge values are shown for deep-sea clays and cherts. The 5 lithologic units associated with each samples have been defined by Plank et al. (2000) and Behl and Smith (1992). Unit I consists of late Miocene to late Pleistocene carbonate-free clays with siliceous microfossils volcanic ash (accounting for 35–50% of the sediment). Unit II (Middle Albian to Early Aptian) consists of dark brown pelagic clays. Unit III is a 104 m thick alternation of radiolarian cherts with porcelanite and siliceous clays. Unit IV comprises 125 m of Upper Valanginian to Upper Hauterivian intercalated radiolarian chert, porcelanite and siliceous chalks or marls (Bartolini, 2003). Unit V is a 125 m thick alteration of cherts and radiolarite sediments capped by volcanoclasitic turbidite of probable Albian age. Dark gray boxes represent the Bulk Silicate Earth (BSE) estimates.

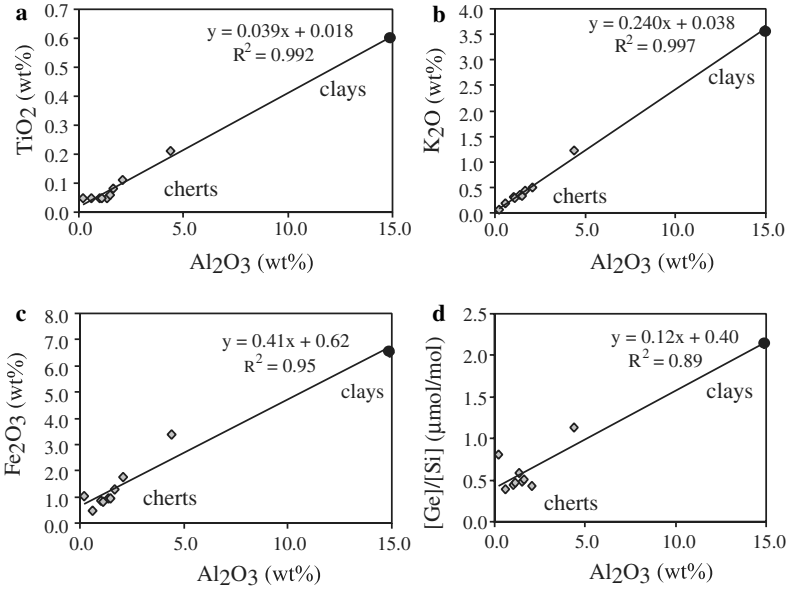

Fig. 8. Correlation between Al_2O_3 and other elements geochemistry such as TiO_2 (a), K_2O (b), Fe_2O_3 (c) and Ge/Si (d) for deep-sea cherts and overlying deep-sea clays at Site 1149 (sample 1149A-20X1,140). The best-fit approximation line for plots (a–c) suggest that clay contamination is the main source of Al, Ti, Fe and K in cherts. Ge concentration is not strongly correlated with clay contamination (i.e., Al_2O_3 concentration) and both high and low-Al cherts may have higher Ge concentrations.

changes in the Ge isotopic composition of the seawater]. However, the overall lack of relationship between δ^{74}Ge and Ge/Si (or 1/[Ge]) values for deep-sea cherts rules out binary mixing for the explanation of the observed 1.3‰ range.

During lithification, the accumulated opal frustules undergo successive dissolution–precipitation–recrystallizations processes from the least ordered opal form (Opal-A) to the crystobalite–tridymite form (opal-CT) and finally to quartz (e.g., Murray et al., 1992). Diagenetic transfor-

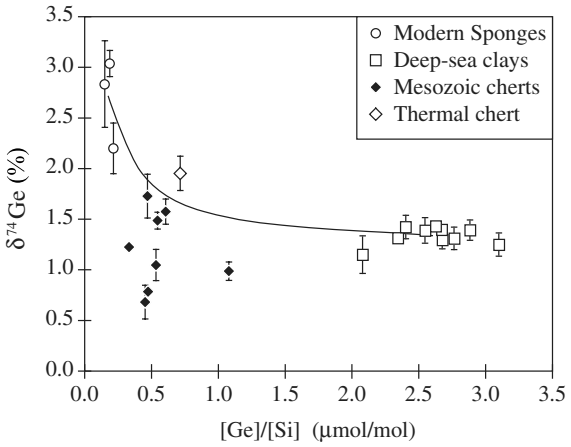

Fig. 9. Ge/Si ratios versus δ^{74}Ge values of Mesozoic deep-sea cherts from ODP Sites 1149 and 801 compared to modern marine sponges and Cenozoic deep-sea clays. Chert values are clearly outside the range defined by a hypothetical mixture (solid line) of diagenetic fluids formed by bulk dissolution of biogenic opal (defined by modern sponges) and clays. An additional source of silica, presumably diagenetic, with δ^{74}Ge values lower than the δ^{74}Ge of the BSE and low Ge/Si ratios is required to explain the range of values for cherts.

mation of clay minerals can also be an accessory source of silica for chertification (Keene and Kastner, 1974). Since sediments at ODP Sites 801 and 1149 have been affected by variable silica mobility (Behl and Smith, 1992; Plank et al., 2000), great potential exist for significant Ge isotope fractionation during diagenesis. It has been suggested that quartz precipitation strongly fractionates Ge/Si ratios at low temperature (Evans and Derry, 2002) and may also fractionate Ge isotopes. Given the very low K_D for Ge in quartz (Evans and Derry, 2002), the value of $\alpha_{\text{quartz-fluid}}$ for Ge isotopes can be estimated by the lowest δ^{74}Ge values of the diagenetic cherts (0.7‰) and is only sensitive to the δ^{74}Ge value of the diagenetic fluid. Using the two extreme isotopic compositions of deep-sea clays and marine sponge for the δ^{74}Ge value of the fluid and a K_D of 0.023 (Evans and Derry, 2002), $\alpha_{\text{quartz-fluid}}$ would range between 0.9975 and 0.9995, which compares well with the size and the scale of the Si isotope fractionation during silica polymorphs transformations (Basile-Doelsch et al., 2005). In addition, Ge(IV) does not undergo reduction to Ge(II) under Earth surface conditions (Capobianco et al., 1999), so Ge isotope fractionation in cherts are certainly not associated with redox reactions but rather related to Ge(IV) incorporation into silica matrix.

One important implication of this result is that, in addition to a sink of light isotopes of Ge associated with iron oxyhydroxide (Galy et al., 2002), the early diagenesis of silica provides an additional mechanism to explain the heavy δ^{74}Ge value of the ocean.

One thermal chert (801B-40R1,2) has been measured and is characterized by the highest δ^{74}Ge value at 2.0‰. As thermal cherts are rocks that were silicified under abnormally high temperature conditions at the proximity of volcanic flows, δ^{74}Ge values might be influenced by hydrothermal silica input at the sediment–basement interface. Although the Ge isotope composition of hydrothermal fluids are presently unknown, it is expected that significant fractionation of Ge isotope may occur during Ge sorption onto Fe oxyhydroxide in altered basalts (Galy et al., 2002) and yielding higher δ^{74}Ge values in the fluid relative to fresh basalt.

6. Conclusions

In this study, we have presented a method for the sensitive and precise determination of Ge isotopic variations by MC-ICP-MS using an on-line HG system. Instrumental mass bias is corrected using the "standard-sample bracketing" method. Important advantages of the use of this method for the determination of Ge isotopes relative to the other alternative methods are: (1) high sensitivity, lowering the total amount of Ge required for one analysis down to 10 ng; (2) analysis of matrix-free samples permit Ge to be separated from potential interferences that may affect instrumental mass bias. Although the HG system is by itself a method to isolate Ge from the geological matrix, a pre-concentration step was always used for accurate analysis. The external precision obtained for the ^{74}Ge/^{70}Ge ratio is 0.2‰ at 95% confidence level and allows identification of natural variations of Ge isotopes.

Among key observations, Ge isotope compositions of crustal rocks and marine deep-sea clays are homogeneous and permit definition of a bulk Earth reservoir with δ^{74}Ge value at 1.3‰. In contrast, chemically and biologically precipitated material such as cherts, glauconite and marine sponges display significantly different δ^{74}Ge values of about 2.5‰. In the absence of a directly determined Ge isotope composition of seawater, modern marine sponges have been used as a preliminary estimate of seawater δ^{74}Ge values. Mesozoic deep-sea cherts have δ^{74}Ge values ranging from 0.7‰ to 2.0‰ and likely result from a combination of processes, such as mixing between igneous (at 1.3‰) and marine sources (>3‰) and Ge isotope fractionation during opal diagenesis.

Given the relatively short residence time of Ge in the oceans (around 10 ky), it has been suggested that the Ge/Si ratio in seawater may vary in response to climatic changes, and in particular during glacial–interglacial changes (Shemesh et al., 1989; Mortlock et al., 1991). With the recognition that glacial–interglacial variations of marine Ge/Si can be attributed either to climatically driven continental weathering process changes (Froelich et al., 1992; Filippelli et al., 2000; Lin and Chen, 2002), or to variations in authigenic outputs to marine sediments via a "missing Ge-sink" (Elderfield and Schultz, 1996; Hammond et al., 2000; King et al., 2000), great potential exist for these to examine secular variations of δ^{74}Ge values in seawater. Therefore, in addition to Si isotopes and Ge/Si tracers, Ge isotopes can offer new insights into the biogeochemical cycles of Ge and Si in the present and past oceans.

Acknowledgments

We thank Stace Beaulieu and Christina De La Rocha for providing the sponge samples. This work benefited from many fruitful discussions with Samia Mantoura and analytical advice from Catherine Pomiès, Mervyn Greaves and Jason Day. Technical support was provided by the STOPFEN-EC Grants (HPRN-CT-2002-0221) and NSF-EAR/IF (0318137). O. Rouxel was supported by a post-doctoral fellowship from the STOPFEN network at Cambridge and the Deep Ocean Exploration Institute at WHOI. This research used samples provided by the Ocean Drilling Program. The ODP is sponsored by the US National Science Foundation (NSF) and participating countries under the management of Joint Oceanographic Institutions (JOI). We gratefully Richard Walker, Clark Johnson, Flip Froelich and one anonymous reviewer for their detailed and constructive reviews which improved the manuscript.

Associate editor: Richard J. Walker

References

Bartolini, A., 2003. Cretaceous radiolarian biochronology and carbon isotope stratigraphy of ODP Site 1149 (Northwestern Pacific, Nadezhda Basin). In: Ludden, J., Plank, T., Escutia, C. (Eds.), *Proc. ODP, Sci. Results*, vol. 185, Ocean Drilling Program, pp. 1–17.

Basile-Doelsch, I., Meunier, J.D., Parron, C., 2005. Another continental pool in the terrestrial silicon cycle. *Nature* **433**, 399–402.

Behl, R.J., Smith, B.M., 1992. Silicification of deep-sea sediments and the oxygen isotope composition of diagenetic siliceous rocks from the western pacific, Pigafetta and east Mariana basins, Leg 129. In: Larson, R.L., Lancelot, Y. (Eds.), *Proc. ODP, Sci. Results*, vol. 129, Ocean Drilling Program, pp. 81–117.

Bernstein, L.R., 1985. Germanium geochemistry and mineralogy. *Geochim. Cosmochim. Acta* **49**, 2409–2422.

Capobianco, C.J., Drake, M.J., de'Aro, J., 1999. Siderophile geochemistry of Ga, Ge, and Sn: cationic oxidation states in silicate melts and the effect of composition in iron–nickel alloys. *Geochim. Cosmochim. Acta* **63**, 2667–2677.

De Argollo, R., Schilling, J.-G., 1978. Ge–Si and Ga–Al fractionation in Hawaiian volcanic rocks. *Geochim. Cosmochim. Acta* **42**, 623–630.

Dedina, J., Tsalev, D.L., 1995. *Hydride generation atomic absorption spectrometry*. Wiley, New York.

De La Rocha, C., 2003. Silicon isotope fractionation by marine sponges and the reconstruction of the silicon isotope composition of ancient deep water. *Geology* **31**, 423–426.

Douthitt, C.B., 1982. The geochemistry of the stable isotopes of silicon. *Geochim. Cosmochim. Acta* **46**, 1449–1458.

Elderfield, H., Schultz, A., 1996. Mid-ocean ridge hydrothermal fluxes and the chemical composition of the ocean. *Annu. Rev. Earth Planet. Sci.* **24**, 191–224.

Evans, M.J., Derry, L.A., 2002. Quartz control of high germanium/silicon ratios in geothermal waters. *Geology* **30**, 1019–1022.

Filippelli, G.M., Carnahan, J.W., Derry, L.A., Kurtz, A., 2000. Terrestrial paleorecords of Ge/Si cycling derived from lake diatoms. *Chem. Geol.* **168**, 9–26.

Froelich, P.N., Andreae, M.O., 1981. The marine geochemistry of germanium—Ekasilicon. *Science* **213**, 205–207.

Froelich, P.N., Blanc, V., Mortlock, R.A., Chillrud, S.N., Dunstan, W., Udomkit, A., Peng, T.-H., 1992. River fluxes of dissolved silica to the ocean were higher during glacials: Ge/Si in diatoms, rivers, and oceans. *Paleoceanography* **7**, 739–767.

Galy, A., Pokrovsky, O.S., Shott, J., 2002. Ge-isotopic fractionation during its sorption on goethite: an experimental study. *Geochim. Cosmochim. Acta* **66**, A259.

Galy, A., Pomiès, C., Day, J.A., Pokrovsky, O.S., Schott, J., 2003. High precision measurement of germanium isotope ratio variations by multiple collector—inductively coupled plasma—mass spectrometry. *J. Anal. At. Spectrom.* **18**, 115–119.

Goldschmidt, V.M., 1958. *Geochemistry*. Oxford University Press, Oxford.

Govindaraju, K., 1994. 1994 compilation of working values and sample description for 383 geostandards. *Geostandards Newslett.* **18**, 1–158.

Green, M.D., Rosman, K.J.R., deLaeter, J.R., 1986. The isotopic composition of germanium in terrestrial samples. *Int. J. Mass Spectrom. Ion Proc.* **68**, 15–24.

Halicz, L., 1990. Germanium contents of selected international geostandards by hydride generation ICP-AES. *Geostandards Newslett.* **14**, 459–460.

Halliday, A.N., Lee, D.-C., Christensen, J.N., Walder, A.J., Freedman, P.A., Jones, C.E., Hall, C.M., Yi, W., Teagle, D., 1995. Recent developments in inductively coupled plasma magnetic sector multiple collector mass spectrometry. *Int. J. Mass Spectrom. Ion Proc.* **146/147**, 21–33.

Hammond, D.E., McManus, J., Berelson, W.M., Meredith, C., Klinkhammer, G.P., Coale, K.H., 2000. Diagenetic fractionation of Ge and Si in reducing sediments: the missing Ge sink and a possible mechanism to cause glacial/interglacial variations in oceanic Ge/Si. *Geochim. Cosmochim. Acta* **64**, 2453–2465.

Hirata, T., 1997. Isotopic variations of germanium in iron and stony iron meteorites. *Geochim. Cosmochim. Acta* **61**, 4439–4448.

Kapusta, Y., Steinitz, G., Akkerman, A., Sandler, A., Kotlarsky, P., Nagler, A., 1997. Monitoring the deficit of ^{39}Ar in irradiated clay fractions and glauconites: Modeling and analytical procedure. *Geochim. Cosmochim. Acta* **61**, 4671–4678.

Keene, J.B., Kastner, M., 1974. Clays and formation of deep-sea chert. *Nature* **249**, 754–755.

King, S.L., Froelich, P.N., Jahnke, R.A., 2000. Early diagenesis of germanium in sediments of the Antarctic South Atlantic: in search of the missing Ge sink. *Geochim. Cosmochim. Acta* **64**, 1375–1390.

Kolodny, Y., Halicz, L., 1988. The geochemistry of germanium in deep-sea cherts. *Geochim. Cosmochim. Acta* **52**, 2333–2336.

Kurtz, A.C., Derry, L.A., Chadwick, O.A., 2002. Germanium-silicon fractionation in the weathering environment. *Geochim. Cosmochim. Acta* **66**, 1525–1537.

Larson, R.L., Lancelot, Y., Shipboard Scientific Party, 1992. *Proc. ODP, Sci. Results*, vol. 129. Ocean Drilling Program, College Station (TX).

Lin, H.-L., Chen, C.-J., 2002. A late Pliocene diatom Ge/Si record from the Southeast Atlantic. *Mar. Geol.* **180**, 151–161.

McManus, J., Hammond, D.E., Cummins, K., Klinkhammer, G.P., Berelson, W.M., 2003. Diagenetic Ge–Si fractionation in continental margin environments: further evidence for a nonopal sink. *Geochim. Cosmochim. Acta* **67**, 4545–4557.

Mortlock, R.A., Charles, C.D., Froelich, P.N., Zibello, M.A., Saltzman, J., Hays, J.D., Burckle, L.H., 1991. Evidence for lower productivity in the Antarctic Ocean during the last glaciation. *Nature* **351**, 220–223.

Mortlock, R.A., Froelich, P.N., 1987. Continental weathering of germanium: Ge/Si in the global discharge. *Geochim. Cosmochim. Acta* **51**, 2075–2082.

Mortlock, R.A., Froelich, P.N., 1996. Determination of germanium by isotope-hydride generation inductively coupled plasma mass spectrometry. *Anal. Chim. Acta* **332**, 277–284.

Mortlock, R.A., Froelich, P.N., Feely, R.A., Massoth, G.J., Butterfield, D.A., Lupton, J.E., 1993. Silica and germanium in Pacific Ocean hydrothermal vents and plumes. *Earth Planet. Sci. Lett.* **119**, 365–378.

Murray, R.W., Brink, M.R.B., Gerlach, D.C., PriceRuss, G., Jones, D.L., 1992. Rare earth, major, and trace element composition of Monterey and DSDP chert and associated host sediment: assessing the influence

of chemical fractionation during diagenesis. *Geochim. Cosmochim. Acta* **56**, 2657–2671.

Plank, T., Ludden, J.N., Escutia, C., Shipboard Scientific Party, 2000. *Proc. ODP, Init Repts.*, vol. 185. Ocean Drilling Program, College Station (TX).

Pokrovski, G.S., Schott, J., 1998. Thermodynamic properties of aqueous Ge(IV) hydroxide complexes from 25 to 350 °C: implications for the behavior of germanium and the Ge/Si ratio in hydrothermal fluids. *Geochim. Cosmochim. Acta* **62**, 1631–1642.

Reincke, T., Barthel, D., 1997. Silica uptake kinetics of *Halichondria panicea* in Kiel Bight. *Mar. Biol.* **129**, 591–593.

Rouxel, O., Dobbek, N., Ludden, J., Fouquet, Y., 2003a. Iron isotope fractionation during oceanic crust alteration (Site ODP 801). *Chem. Geol.* **202**, 155–182.

Rouxel, O., Ludden, J., Carignan, J., Marin, L., Fouquet, Y., 2002. Natural variations of Se isotopic composition determined by Hydride Generation Multiple Collector Coupled Mass Spectrometer. *Geochim. Cosmochim. Acta* **66**, 3191–3199.

Rouxel, O., Ludden, J., Fouquet, Y., 2003b. Antimony isotope variations in natural systems and implications for their use as geochemical tracers. *Chem. Geol.* **200**, 25–40.

Shemesh, A., Mortlock, R.A., Froelich, P.N., 1989. Late cenozoic Ge/Si record of marine biogenic opal: implications for variations of riverine fluxes to the ocean. *Paleoceanography* **4**, 221–234.

Shima, M., 1963. Isotopic composition of germanium in meteorites. *Geochim. Cosmochim. Acta* **27**, 4289–4292.

Xue, S., Yang, Y.-L., Hall, G.S., Herzog, G.F., 1997. Germanium isotopic compositions in Canyon Diablo spheroids. *Geochim. Cosmochim. Acta* **61**, 651–655.

Yokoyama, T., Makishima, A., Nakamura, E., 1999. Evaluation of the coprecipitation of incompatible trace elements with fluoride during silicate rock dissolution by acid digestion. *Chem. Geol.* **157**, 175–187.